Three-dimensional modelling of the rock breakage process

H.Y. Liu
Golder Geomechanics Centre, the University of Queensland, QLD4067, Australia

F. Alonso-Marroquin
MoSCoS, the University of Queensland, QLD4067, Australia

D.J. Williams
Golder Geomechanics Centre, the University of Queensland, QLD4067, Australia

W.D. Guo
Department of Civil Engineering, Griffith University, QLD4222, Australia

ABSTRACT: The progressive failure model is implemented into the commercial finite element code ABAQUS for 3D modeling of rock breakage process. In order to facilitate the usage of such implementation, a software package TUNGEO3D is developed using C++, OpenGL, Fortran and Python script to integrate the pre-processing, the subroutines and procedures interacting with ABAQUS, and post-processing. Several examples are presented to verify such implementation and demonstrate the benefits of the implementation.

1 INTRODUCTION

In recent years, the two-dimensional (2D) progressive failure model has emerged as a powerful numerical procedure for the analysis of crack problems in heterogeneous brittle materials (Tang, 1997; Liu, 2004). It has been widely acknowledged that the method eases from crack initiation and propagation modelling till structure failure modelling under the framework of damage mechanics (Liu et al., 2007 and 2008). In this paper, the 2D progressive failure model will be extended to 3D and be implemented into the general finite element code ABAQUS with its user-defined subroutine options to develop a three-dimensional (3D) code for tunneling and Geomechanics (TUNGEO3D). ABAQUS has been proved to be useful for stress analysis but can not simulate heterogeneous brittle failure. Through this implementation, the user can benefit from the many built-in features of ABAQUS, including some of the pre- and post-processing options and interface modeling, to perform breakage modelling. This paper focuses on the implementation aspects for the 3D modelling of the breakage process in heterogeneous brittle materials to develop the TUNGEO3D code.

2 TUNGEO3D

In comparison to the general finite element method such as ABAQUS, the progressive failure model provides significant benefits in the numerical modelling of the brittle material failure.

2.1 *Heterogeneous material model*

The microstructure of rock is more or less heterogeneous. The failure behaviour of rock under loading is strongly influenced by this heterogeneous microstructure. Consequently, the numerical method for modelling the rock failure should take the heterogeneity into consideration. On the basis of previous work, rock heterogeneity can be characterized with Weibull satistical approaches in the numerical model. The Weibull probability distribution function can be expressed as the following

$$f(\sigma)=\frac{m}{\sigma_0}\left(\frac{\sigma}{\sigma_0}\right)^{m-1}\exp\left[-\left(\frac{\sigma}{\sigma_0}\right)^{m}\right] \tag{1}$$

where σ = the elemental parameter; m = the shape parameter describing the scatter of σ, is defined as the homogeneous index (Tang, 1997); and σ_0 = the mean elemental parameter. In numerical simulation, a finite element network model is built, in which elemental parameters, such the critical strength σ_c, the elastic modulus E, etc follow the weibull distribution low with the homogeneous index m and seed parameters σ_{c0}, E_0, etc. The special random microstructure of heterogeneous rock can be reflected by the disorder of the mesoscopic structure, which is achieved by Monte Carlo method. The cumulative probability function of Weibull distribution is

$$P(\sigma)=\int_0^{\sigma} f(\sigma)d\sigma=1-\exp\left[-\left(\frac{\sigma}{\sigma_0}\right)^{m}\right] \tag{2}$$

The random data between 0 and 1 generated by the Monte-Carlo method has a certain value in the cumulative distribution function $P(\sigma)$. The corresponding value σ is given to elements. Therefore, the method based on statistics and randomicity satisfies the requirements of heterogeneity and randomic-

ity of element parameters in the finite element network of rock materials.

The heterogeneity in a brittle material is intimately related to the defects statistics, e.g. micro-pores and micro-cracks. When the rock is loaded, one or several of the larger defects in the rock are caused to propagate. In a typical defect size distribution observed in heterogeneous rock, the extremal size distribution of defects larger than a certain size a_1 can be fitted using the distribution function of the Cauchy type

$$g(a)=\left(\frac{q^*}{a}\right)^z \tag{3}$$

where a is the half-length of defects, q^* is the extremal parameters, and z is defect size distribution shape index or called fractal index. After a series of transformation performed by Wong et al. (2006), the probability that the defects in a larger volume, V, are larger than a_1 can be expressed

$$P=1-\exp\left[-V\int_{a_1}^{\infty} g(a)da\right]=1-\exp\left[-\frac{V}{V_0}\left(\frac{a'}{a_1}\right)^{z-1}\right] \tag{4}$$

where V_0 is the elemental volume and a' is a length scale defining the lower limit of crack length described by the power law. By applying the fracture mechanics relation $K_{IC}=Y\sigma\sqrt{\pi a}$, the cumulative probability that failure develops at stresses less than σ is given by

$$P(\sigma)=1-\exp\left[-\frac{V}{V_0}\left(\frac{\sqrt{\pi a'}\,\sigma Y}{K_{IC}}\right)^{2z-2}\right] \tag{5}$$

Therefore, by comparing the integral distribution function of Weibull's distribution and the equation describing the probability that fracture occurs under a certain stress, the homogeneous index and seed parameter in the heterogeneous material model relate to the rock microstructure by

$$m=2z-2 \tag{6}$$

$$\sigma_0=\left(\frac{V}{V_0}\right)^{-\frac{1}{m}}\frac{K_{IC}}{Y\sqrt{\pi a'}} \tag{7}$$

Using this method, Liu et al. (2005 and 2006) successfully obtained the homogeneous indices and seed parameters of LKAB's Kiruna managnites and three types of granites (Avja, LEP and Vandle) taken from three quarries near Stockholm in Sweden.

2.2 *MC and unified strength criteria*

The Mohr-Coulomb (MC) strength criterion is one of the most widely used strength criteria in geotechnical engineering application, including rock engineering modelling and design. In terms of principal stresses, the Mohr-Coulomb strength criterion can be expressed as the following

$$F=\sigma_1-\sigma_3\frac{1+\sin\phi}{1-\sin\phi}-\frac{2c\cos\phi}{1-\sin\phi} \tag{8}$$

where c is the cohesion and ϕ is the angle of internal friction. In order to avoid the tip angle in the tension area of the Mohr-Coulomb strength criterion, it is modified to include the tension cut-off when $\sigma_3<0$, i.e. under tensile stress, it is assumed that failure occurs when the tensile stress reaches the tensile strength

$$F=\sigma_3-\sigma_t \tag{9}$$

However, MC criterion is only valid for the brittle part of the rock failure envelope and has not taken the effect of intermediate principal stress into account. Under 3D conditions, a nonlinear unified strength criterion proposed by Yu et al. (2002) is used:

$$F=\sigma_1-\frac{1}{1+b}(b\sigma_2+\sigma_3)-\sigma_c\left[\frac{m}{(1+b)\sigma_c}(b\sigma_2+\sigma_3)+s\right]^{\alpha} \tag{10}$$

$$F'=\frac{1}{1+b}(b\sigma_2+\sigma_1)-\sigma_3-\sigma_c\left[\frac{m}{\sigma_c}\sigma_3+s\right]^{\alpha} \tag{11}$$

where σ_c is the uniaxial compressive strength of an intact rock material; σ_1, σ_2 and σ_3 are the maximum, intermediate and minimum principal stresses, respectively; m, s and α are the same material parameters as those in the Hoek-Brown criterion; and b is the intermediate stress parameter, which varies from 0 to 1. When $F\geq F'$, Eq. 10 is used, otherwise, Eq.11 is referred. When $b=0$, the nonlinear unified strength criterion simplifies to the Hoek-Brown criterion, a single-shear strength criterion that forms the lower bound. When $b=1$, the nonlinear unified strength criterion simplifies to a nonlinear twin-shear strength criterion that forms the upper bound. According to Yu et al. (2002), all of the strength criteria ranging from the Hoek-Brown criterion (the lower bound) to the nonlinear twin-shear criterion (the upper bound) and the series of criteria ranging between these two bounds may be introduced by a nonlinear unified strength criterion.

2.3 *Mechanical damage model and seismicity*

As observed in experimental studies, a descending elastic modulus and a descending load bearing capacity after a certain stage are the prominent characteristics of rock under loading. Therefore, it is natural to use the damage mechanical model to study the progressive microcracking process in the rock breakage by degrading the elasticity of the rock ma-

terial. Before satisfying the strength criterion described in Section 2.2, the stress and strain follow hook's law

$$\Delta\sigma_{ij} = \lambda\delta_{ij}\Delta\varepsilon_{kk} + 2u\Delta\varepsilon_{ij} \tag{12}$$

After the stresses of the element satisfy the strength criterion, a damage variable D is introduced to describe the degradation of the elemental stiffness according to damage mechanics.

$$D = \frac{A_D}{A} \tag{13}$$

where A_D is the damaged surface area and A is the whole surface area of the representative volume element. Correspondingly, the consitutive relation can be expressed as

$$\Delta\sigma_{ij} = C^D_{ijkl}\Delta\varepsilon^{el}_{kl} = (1-D)C_{ijkl}\left(\Delta\varepsilon_{kl} - \Delta\varepsilon^{pl}_{kl}\right) \tag{14}$$

Under uniaxial tensile stress, tensile damage occurs when the minor principal stress in the element reaches its tensile strength. The tensile damage evolution can then be expressed as:

$$D = \begin{cases} 0 & \varepsilon < \varepsilon_{t0} \\ 1 - \dfrac{\lambda\varepsilon_{t0}}{\varepsilon} & \varepsilon_{t0} \le \varepsilon < \varepsilon_{tu} \\ 1 & \varepsilon \ge \varepsilon_{tu} \end{cases} \tag{15}$$

where λ is the residual strength coefficient. ε_{t0} is the tensile strain at the elastic limit, which is the so-called tensile threshold strain. ε_{tu} is the ultimate tensile strain, which indicates that elements will be completely damaged when the tensile strain attains it. The ultimate tensile strain is usually defined as $\varepsilon_{tu} = \eta\varepsilon_{t0}$, where η is the ultimate tensile strain coefficient. Under multiaxial tensile stresses, the damage variable can be easily obtained by substituting the strain for an equivalent strain. Under uniaxial compressive stress, shear damage occurs when the stresses of the element satisfy the strength criteria described in Section 2.2. The shear damage variable can be described as

$$D = \begin{cases} 0 & \varepsilon < \varepsilon_{c0} \\ 1 - \dfrac{\lambda\varepsilon_{c0}}{\varepsilon} & \varepsilon_{c0} \le \varepsilon < \varepsilon_{cc} \end{cases} \tag{16}$$

where ε_{c0} is the compressive strain at the elastic limit, which is the so-called compressive threshold strain. ε_{cc} is the re-compaction compressive strain, which is usually defined as $\varepsilon_{cc} = \xi\varepsilon_{c0}$, where ξ is the so-called re-compaction compressive strain coefficient. Under multiaxial compressive stress, the shear damage variable is described in detail in a previous thesis (Liu, 2004).

It is assumed that the strain energies released by damaged elements are all in the form of AE. Therefore, the AE energy release can be calculated as

$$\Delta e_i = e_{ic} - e_{ir} \tag{17}$$

where i is the element number, e_{ic} is the elemental strain energy before failure and e_{ir} is the elemental strain energy after failure.

$$e_{ic} = \frac{\left(\sigma_{i1}{}^2 + \sigma_{i2}{}^2 + \sigma_{i3}{}^2 - \sigma_{i1}\sigma_{i3} - \sigma_{i1}\sigma_{i2} - \sigma_{i2}\sigma_{i3}\right)}{2E_i}V_i \tag{18}$$

$$e_{ir} = \frac{\left(\sigma'_{i1}{}^2 + \sigma'_{i2}{}^2 + \sigma'_{i3}{}^2 - \sigma'_{i1}\sigma'_{i3} - \sigma'_{i1}\sigma'_{i2} - \sigma'_{i2}\sigma'_{i3}\right)}{2E'_i}V_i \tag{19}$$

where E_i and E'_i are the elastic moduli of the element before and after failure, respectively; σ_{i1}, σ_{i2} and σ_{i3} are the major, medium and minor principal stresses when the element fails, respectively; σ'_{i1}, σ'_{i2} and σ'_{i3} are the major, medium and minor principal stresses after the element fails, respectively; and V_i is the elemental volume.

2.4 *Implementation in ABAQUS*

Implementing the progressive failure model into the general finite element code ABAQUS does imposes certain restrictions, but it also provides access to many of the available features of such a code. From a typical ABAQUS input file, *.inp (input file), the nodal coordinates and mesh topology are saved as ASCII files. A routine reads the nodal coordinates and mesh topology. Through the *USER MATERIAL command, a user subroutine UMAT_TUNGEO is called, where we define the homogeneous indices, seed parameters, residual strength coefficient, ultimate tensile strain coefficient, ultimate compressive strain coefficient, etc. The subroutine heading and variable declarations follow the ABAQUS conventions. In addition, a series of subroutines is written inside the UMAT_TUNGEO subroutine to incorporate the core of the progressive failure model, which includes HOMO for heterogeneous material model, CRIT for MC and unified strength criteria, and DAMG for the mechanical damage model and associated seismicity. In UMAT_TUNGEO, after initializing some vectors and matrices, HOMO is called if the material is set to be heterogeneous. It generates random numbers following Monte-Carlo method and assign material properties to elements following the Weibull distribution. The routine CRIT is then called to check if the computed stresses satisfy the strength criteria. If it is, the material will be damaged and the routine DAMG is called to calculate damage variables and update damaged material properties. Finally, output settings are specified. User materials have limited capabilities in ABAQUS and some of variables can not be output to the *.odb (output database) file for plotting purposes. In this case, they are output to *.dat file for checking purpose and *.fil (binary results file) for further post-

processing in TUNGEO3D. For running an analysis including the user subroutine, the execution procedure is of the following form ABAQUS JOB = <INPUT FILE NAME> USER = UMAT_TUNGEO.

In order to link all of modules introduced above together, TUNGEO3D is developed using ABAQUS as a framework. During numerical simulation, firstly the numerical model is built according to the heterogeneous material model with the homogeneous index, and the seed parameters. Then in order to perform the finite element analysis, the other parameters are specified for the numerical model, and the initial boundary conditions are applied to it. Following this procedure, the elements are brought to the equilibrium state under the initial boundary conditions. After that, a stress disturbance is applied to the numerical model, which may be caused by force loading, displacement loading or stress redistribution. ABAQUS/Standard (may include ABAQUS/Explicit in future) is used to calculate the stress and strain distributions in the finite element network because of the stress disturbance. The calculated stresses are substituted into the Mohr-Coulomb or unified strength criterion to check whether or not damage occurs. If the strength criterion is not satisfied, the external loading is increased further. Otherwise, the element is damaged and becomes weak according to the rules specified by the mechanical damage model, which results in a new perturbation. The stress and deformation distributions throughout the model are then adjusted instantaneously after each rupture to reach the equilibrium state. Due to the new stress disturbances, the stress of some elements may satisfy the critical value and further ruptures are caused. The process is repeated until no failure elements are present. The external load is then increased further. In this way the system develops a macroscopic fracture. Thus the code links the mechanical damage model to the continuum damage model and ultimately to macrostructure failure, which has been regarded as one of the most challenging tasks in the area of brittle failure micromechanics. Energy is stored in the element during the loading process and is released as acoustic emission through the onset of elemental failure. Due to the interaction induced by stress redistribution and long-range deformation, a single important element failure may cause an avalanche of additional failures in neighbouring elements, leading to a chain reaction releasing more energies.

In order to make its use more convenient, a user-friendly pre- and post-processor is also developed and integrated into the TUNGEO3D code using Visual C++ (VC), OpenGL, Fortran and ABAQUS's Python script to generate the finite element mesh (although more complicated finite element models are usually imported from ABAQUS/CAE), prepare the input data, and visually display the calculated results. VC is a powerful and complex Object-Oriented Programming (OOP) Integrated Development Environment (IDE) tool for building 32-bit applications in a Windows environment. With its code-generating wizards, it can produce the shell of the TUNGEO3D code in seconds. The visual editing tool makes the layout of menus and dialogs in the TUNGEO3D code a snap. Through the Windows Graphic Device Interface and OpenGL, it is easy to develop a module for the TUNGEO3D code to design the geometrical models for mechanical tool and objects with various irregular shapes, and then fill them with different material properties. Using the AppWizard and ClassWizard, the TUNGEO3D code is designed to support the complicated data structure or even databases to organize a large number of data, as well as Object Linking and Embedding (OLE, also known as ActiveX) to exchange data with an external executable program. Moreover, MFC's (Microsoft Foundation Class) document/view architecture separates the data in the TUNGEO3D code from the way in which the user actually views and manipulates. Simply, the document object is responsible for storing, loading, and saving the data, whereas the view object enables the user to see the data on screen and to edit that data in a way that is appropriate to the TUNGEO3D code.

3 NUMERICAL EXAMPLES

Several numerical examples are presented in this section to demonstrate the benefits of the proposed TUNGEO3D code. In order to assess the accuracy of the proposed code, the rock breakage processes in the uniaxial compressive strength (UCS) test and the Brazilian tensile strength (BTS) test are firstly modeled and compared with those well documented in literatures. After that, the TUNGEO3D code is used to investigate the rock breakage process induced by rock-concrete interaction, which has huge applications in the design of tunnel lining (e.g. Malmgren and Nordlund, 2008), rock bolts (e.g. Li and Stillborg, 1999), rock socket pile (e.g. Seol et al., 2009), rock joints (e.g. Seidel and Haberfield, 2002), footing and so on.

3.1 *3D modeling of rock breakage process in the UCS and BTS tests*

The numerical model for the UCS test is built according to the geometry suggested by ISRM, i.e. the diameter is 54mm and the ratio between the height and the diameter is 2.5. In order to verify the numerical code, both 2D and 3D modellings are conducted. In the 2D modeling, the UCS test is simplified as a plane stress problem and a vertical section is considered. In both cases, the load at a constant displacement increment of 0.002 mm per step is applied in the vertical direction. The specimens are loaded up to failure, and the complete force-displacement curves are recorded.

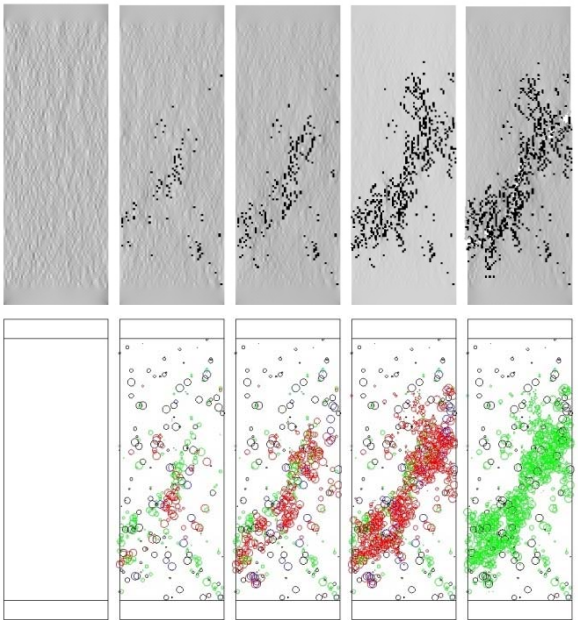

a) 2D (Up: major principal stress, down: acoustic emission)

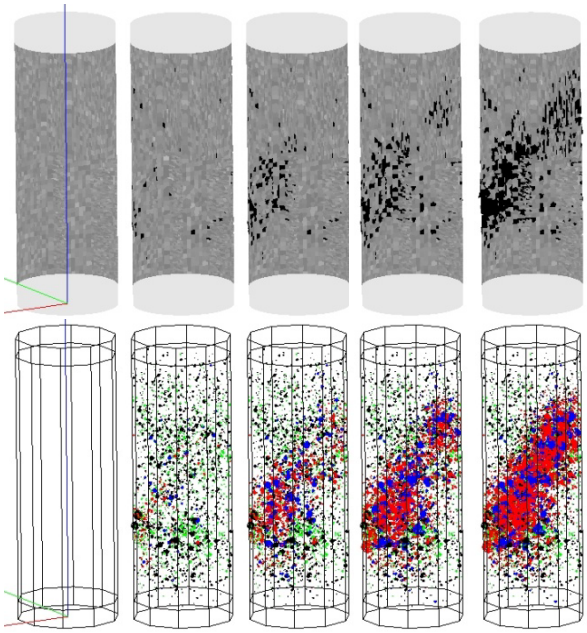

b) 3D (Up: major principal stress, down: acoustic emission)

Figure 1. 2D and 3D modelling of the rock breakage process in the UCS test

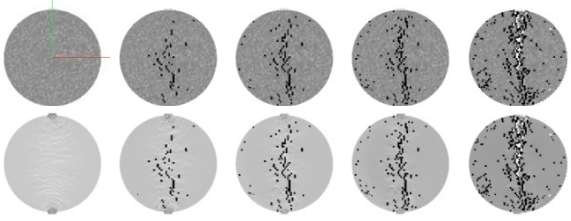

a) 2D (Up: elastic modulus, down: major principal stress)

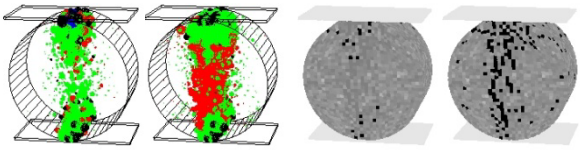

b) 3D (left: acoustic emission, right: elastic modulus)

Figure 2. 2D and 3D modelling of the rock breakage process in the BTS test

Figure 1 shows the simulated initiation, propagation and coalescence of the fractures at different loading levels. For the 2D modeling, the distributions of the major principal stress and acoustic emission are depicted. For the 3D modeling, the evolutions of the elastic modulus and acoustic emission are recorded. It can be seen that in both 2D and 3D modeling, the onset of failure is indicated by the formation of a large number of isolated microfractures and then the microfractures begin to cluster and become clearly localized. This is quickly followed by the development of a macroscopic fracture which split the specimen along an approximately 45-degree plane. It can be seen that the main mechanism is tensile failure from the recorded acoustic emissions, where tensile failures in current step are marked using red colour and those in previous step are depicted using green color; compressive failures in current step are marked using blue color and those in previous step are depicted using black color; and the radii of the circle and sphere represent the sizes of the released energies. From above descriptions, it can be seen that the modeled progressive failure process and failure mechanism are consistent with those in rock mechanics textbooks.

As shown in Figure 2, the recorded failure processes in both 2D and 3D numerical tests of the Brazilian tests indicate the macroscopic cracks start at some point near the central line of the discs and propagate radially outward giving rise to a diametral fracture plane with many small branches.

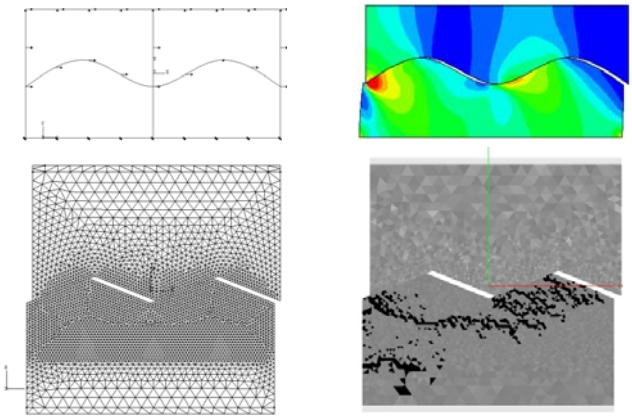

a) 2D (Up: elastic analysis where rock and concrete are assumed to be homogeneous, down: breakage analysis, where heterogeneous is assumed)

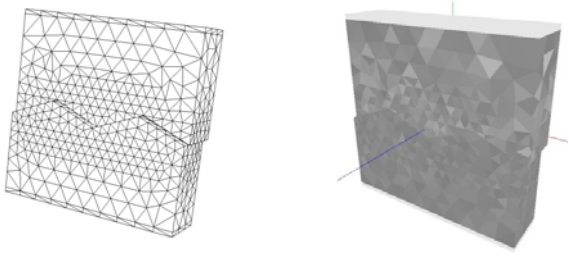

b) 3D (Left: finite element mesh, Right: elastic modulus)

Figure 3. 2D and 3D modelling of the rock breakage process induced by rock-concrete interaction

3.2 *3D modeling of the rock breakage process induced by rock-concrete interaction*

This numerical example demonstrates the benefits of such kind of implementation, which uses the interface modeling technique available in ABAQUS to model the rock breakage process induced by rock-concrete interaction. It is well known that conventional finite element analysis presents some difficulties at large strain. Since nodal compatibility is enforced, no relative displacement is permitted between the rock and contact and hence very large shear strain expected at the interface. Consequently it is difficult for the finite element code to model the interaction between rock and concrete. The ABAQUS interface modeling technique use a slip element to simulate slippage at the rock-concrete interface on the basis of the master-slave formulation.

The friction between the rock and concrete is then modeled using an isotropic Coulomb model, where a friction coefficient and a stress limit is introduced to control the finite-sliding between the master and slave surfaces

$$\tau = \mu p \tag{20}$$

where μ is the friction coefficient and p is the contact pressure. The shear stress transmitted between the two surfaces is computed by multiplying the normal force across the interface by the friction coefficient between the surfaces. The limiting shear stress $\tau_{\max}$ at the rock-concrete interface is a function of shear strengths of rock and concrete. The contact between master and slave surfaces is established using a contact search algorithm, which uses both global and local search procedures to provide accuracy and computational efficiency. The global search computes the distance from each slave node to the master surface elements and chooses the master surface node nearest to the slave surface node. During the local searches, a slave node searches only those elements attached to the tracked master surface node and only the closest master surface node is chosen.

The model results are depicted in Figure 3. It can be seen that a curved failure surface develops from the loading asperity and approximately intersect the trailing face of the asperity. The geometry of the modeled failure surface is consistent reasonably well with the closed-form solution of Sokolovsky and laboratory test results described by Seidel and Haberfield (2002).

4 CONCLUSIONS

In this paper, the progressive failure model developed by us in previous studies is implemented into the commercial finite element code ABAQUS. The implementation is based on the user subroutine UMAT and enables the 3D modeling of heterogeneous brittle material breakage process. To facilitate the usage of such implementation, a software package called TUNGEO3D, a three dimensional code for tunnelling and geomechanics, is developed using Visual C++, OpenGL, Fortran and ABAQUS's Python script to integrate the pre-processing, the subroutines and procedures interacting with ABAQUS finite element analyzer and post-processing. Rock breakage processes in UCS, BTS and induced by rock-concrete interaction are modeled using TUNGEO3D to verify the implementation and demonstrate the benefits of such implementation. It seems that the results are promising.

5 ACKNOWLEDGEMENTS

The first author would like to thank Prof. Chun'an Tang, Prof. Shaoquan Kou and Prof. Per-Arne Lindqvist for their supervisions during the developments of the realistic failure process analysis (RFPA2D) code and the rock-tool (RT2D) interaction code, which form the basis of the 3D code for tunnelling and geomechanics (TunGeo3D) used in this study.

6 REFERENCES

ABAQUS. 2001. ABAQUS/Standard User's Manual. Hibbitt, Karlsson & Sorensen, Inc.

Li, C., Stillborg, B. 1999. Analytical models for rock bolts. *Int. J. Rock Mech. Min. Sci.* 36: 1013-1029

Liu, H.Y. 2004. Numerical modeling of the rock fragmentation process by mechanical tools. *Doctoral thesis 32D*, Lulea University of Technology, Sweden

Liu, H.Y., Kou, S.Q., Lindqvist, P.A., Lindqvist, J.E., Åkesson, U., Jacobsson, L., Evertsson, M. & Svedensten, P. 2005. Characterization of ore fragmentation properties in LKAB's Kiruna mine. *LKAB project report*, Sweden

Liu, H.Y., Lindqvist, P.A. Kou, S.Q., Lindqvist, J.E. & Åkesson, U. 2006. Microscope rock texture characterization and simulation of rock aggregate properties. *SGU project report*, Sweden

Malmgren, L. & Nordlund E. 2008. Interaction of shotcrete with rock and rock bolts – a numerical study. *Int. J. Rock Mech. Min. Sci.* 45: 538-553

Seidel, J.P. & Haberfield, C.M. 2002. A theoretical model for rock joints subjected to constant normal stiffness direct shear. *Int. J. Rock Mech. Min. Sci.* 39: 539-553

Seol, H., Jeong, S. & Kim Y. 2009. Load transfer analysis of rock-socketed drilled shafts by coupled soil resistance. *Computers and Geotechnics* 36: 446-453

Tang, C.A. 1997. Numerical simulation of progressive rock failure and associated seismicity. *Int. J. Rock Mech. Min. Sci.* 34: 249-262

Wong, T.F., Wong, R.H.C., Chau, K.T. & Tang, C.A. 2006. Microcrack statistics, Weibull distribution and micromechanical modelling of compressive failure in rock. *Mechanics of Materials* 38: 644-681

Yu, M.H., Zan, Y.W., Zhao, J. & Mitsutoshi, Y. 2002. A unified strength criterion for rock material. *Int. J. Rock Mech. Min. Sci.* 39: 975-989